VERSATILE ELECTRO-DYNAMIC TETHERS DYNAMICS SIMULATOR FOR DEBRIS MITIGATION TOOLS DESIGN

Amedeo Rocchi[(1)], Michèle Lavagna[(2)]

[(1)] Aerospace Science and Technology Department, Politecnico di Milano, Via La Masa 34, 20156 Milano, Italy, amedeo.rocchi@mail.polimi.it
[(2)] Aerospace Science and Technology Department, Politecnico di Milano, Via La Masa 34, 20156 Milano, Italy, michelle.lavagna@polimi.it

ABSTRACT

As far as the space debris mitigation is concerned, the electro-dynamic tethers (EDTs) represent a valuable alternative for de-orbiting. The paper presents a high accuracy numerical simulator developed to support the design and verify the effectiveness of such systems: accurate models are exploited for the mechanical, electrodynamical and environmental representation. Results confirmed the known instabilities of EDTs; to cope with them a control strategy is here proposed, traded off among different laws. The selected control relies on varying either the load resistance or the cathodic emitter voltage drop, at the system cathode, being the current profile the controlled variable. The sensitivity analysis, run on several design parameters, is presented and the interdependencies with stability and performance are discussed.

1. INTRODUCTION

Electrodynamic tethers (EDTs) are cables exploited to exchange energy and/or momentum with the surrounding environment. Their working principle is simple: their relative motion inside the Earth magnetic field induce a motional electric field in the material the tether is made of; the charged particle motion creates a voltage difference along the tether; the electrons collected and re-emitted in the ionosphere allow a current to flow along the tether; the interaction of current and external magnetic field creates a distributed Lorentz force on the tether and the masses it connects, force which opposes to the orbital velocity.
EDTs can be integrated to build up a simple system devoted to mitigation, containing significantly this on board package mass. They can be conceived as plug and play systems on the LEO satellite to dispose, with no energetic input required from the main spacecraft.
Even though EDTs are conceptually simple, they exhibit strongly non-linear behaviors, both dynamically and electrically. They are also strongly susceptible to environmental conditions variations: as an example, the Sun radiation variation affects the tether temperature, which, in its turn, is involved in the tether conductivity. Last, but not least, the electrodynamic forces give rise to a destabilizing torque that, together with the tether flexibility, makes the system prone to instability: a control is usually required.
The possible influence of the tether high flexibility on the control effectiveness was never analyzed in detail previously, since either an accurate control was used on simple tether models (such as dumb-bell model in [1,2,3]) or, vice versa, a very simple control was used on accurate tether models (see [4,5]). A precise simulator is hence required to understand deeply the system dynamics, to study the effects of design choices on performance and stability and to investigate the effectiveness and the efficiency of different control strategies, always taking into account the flexibility of the system.

2. SYSTEM MODELS

The EDT under analysis is considered during its active phase, already deployed and ready for the de-orbiting operation. The system to be simulated is then constituted by the main debris to be de-orbited (it can either be a satellite, a rocket body or another massive object), an end-mass used to deploy the EDT, and the tether itself, connecting the two extended bodies. Fig.1 reports the representation of the overall system and its relevant quantities: the Lorentz force $\boldsymbol{F_l}$, the main body orbital velocity $\boldsymbol{v}$, the local Earth magnetic field $\boldsymbol{B}$, the current I and the electron e^- are shown.

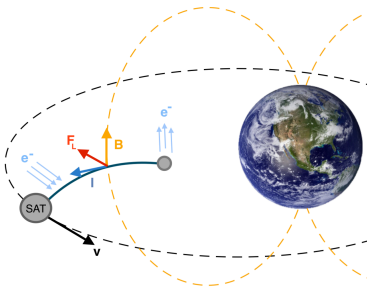

Figure 1. EDT system sketch.

The EDT dynamics modeling within the space environment entails the harmonization of different disciplines modeling: first of all, different

environmental quantities must be modeled, such as the magnetic field, the atmosphere density, the plasma flux; the mechanics of a stack connected by a flexible element has to be reproduced, as well as the electrodynamics; since the electrical properties of the tether are strongly dependent on its temperature, also a thermal model is required. It is here remarked that, the whole disciplinary models have to be harmoniously tuned to get the same level of accuracy in the overall phenomenon simulation.
The numerical simulator core is based on the MUST tool, a *Simulink* toolbox based on the *SimMechanics* environment developed by Politecnico di Milano under ESA contract [6,7], to deal with dynamics of multi-body flexible systems in space. Modules have been developed and plugged to enhance MUST performance to deal with EDT systems analysis and design. In the followings the new modules are presented in detail; existing and exploited modules are briefly recalled. Details are given in [8,9].

2.1. Mechanical Model

To be accurately represented, the tether dynamics must take into account its flexibility, elasticity and damping: neglecting such properties can affect the stability behavior and prevents from results finer than a preliminary analysis. As in [10,4], a lumped parameters representation is here applied and the tether is represented as a series of elastic non-flexible rods. End-masses are modeled as massive extended bodies with 6 dof, and the body-to-tether connection point is user defined.

2.2. Thermal Model

The thermal model is used to evaluate the temperature of the tether to estimate its instantaneous conductivity, required for the current profile computation. The simple model assumes a constant temperature for the whole tether and no heat exchange occurrence between the tether and the end-masses. The Sun, the Earth radiation and albedo and the Joule effect - because of the current - are assumed as external and internal sources respectively, and deep space as sink. The temperature is then the result of a dynamical model, which accounts for the thermal capacity of the overall tether.

2.3. Electrodynamical Model

Constant current tethers or bare tethers with a current profile can be modeled; in the latter alternative, EDT is uncoated and exploited as anodic contactor, to collect electrons from ionosphere. This solution was first conceived in [11]. The bare EDT case is not trivial: a fast semi-analytical method proposed in [12], is here exploited to compute the current profile. The assumption of rectilinear tethers is here relaxed, to exploit the model while preserving the cable flexibility: the motional electric field along the tether E_t is corrected with a factor L^*/L, being L^* the length of the projection of the tether along its end-points connecting line and L the total tether length (see fig. 2): as a consequence, the electric field component along the tether is decreased whenever the tether assumes, because of the dynamics, a non-rectilinear shape.

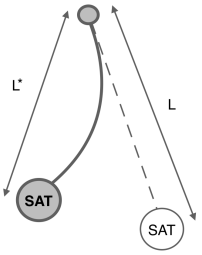

Figure 2. Non-rectilinear condition sketch.

An example of the current profiles obtained in the ideal case of rectilinear tethers with varying cathodic load Z_l is reported in fig. 3. The varying cathodic load can be exploited to tune the control, as discussed in sec.7.

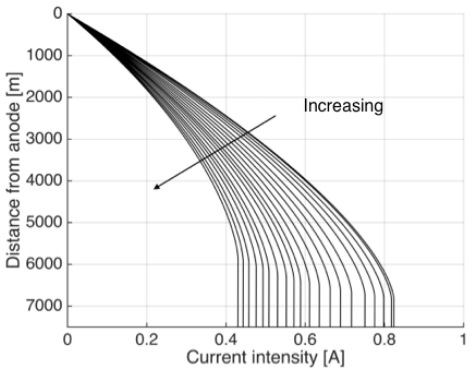

Figure 3. Current profile example.

For the particular case in which the bare tether is used both as anodic and cathodic contactor (useful for nano-satellites, as proposed in [13]), the governing equations reported in [12] are solved with the appropriate boundary conditions: null voltage difference at the cathodic end is imposed. To this end, the tether resistance contribution to the current profile is neglected, which is verified for short tether and relatively low current. The current is evaluated at m positions along the tether length, being m much higher than the number of tether discretization elements. Lorentz force for each point along the tether is computed according to eq. 1 and applied to the closest node mass; in eq.1, $\boldsymbol{F_{dl_i}}$ is the Lorentz force vector acting on the ith portion of tether, $\boldsymbol{dl_i}$ is a vector having as modulus the length of the ith tether discretization element, and supported by the tether discretization element orientation in space; I_i is the current flowing inside the ith tether element and $\boldsymbol{B}$ is the magnetic field vector.

$$\boldsymbol{F_{dl_i}} = I_i(\boldsymbol{dl_i}\times\boldsymbol{B}) \qquad \text{i=1,…,m} \qquad (1)$$

Couples are then introduced in order to take into account also the contributions due to non-uniform current distribution across tether elements which can be seen as localized electrodynamic torques.

3. ENVIRONMENTAL AND PERTURBATIONS MODELS

The context of the current study is the LEO space debris disposal, therefore the environment significant effects are limited to such a space region: atmospheric models for drag estimation, non-uniform mass distribution models for precise gravity effects, magnetic field and ionosphere models for the electrodynamic interaction have been plugged into the tool.

3.1. Drag and Atmospheric Density

The drag force is computed for each tether element and the satellite body; whenever a tape tether (rectangular section) is considered each tether element surface is evaluated as $\frac{2}{\pi}wl$ to take into account possible torsion, as done in [13] (being w the tether width; l the tether element length). Two atmospheric models are available, depending on the needed accuracy: the high accuracy *NRLMSISE-00* [14], and the simpler model presented in [15].

3.2. Gravitational Field and Force

The gravitational force acting on the orbiting stack is evaluated as the gradient of a high order (up to 120th) spherical harmonic expansion of the gravitational potential. Whenever required, the high order potential can be neglected, leaving only the term which leads to keplerian orbits.

3.3. Magnetic Field

A correct reconstruction of the local magnetic field vector is crucial for motional electric field and Lorentz forces estimation. The magnetic field tilt, which has always a very important influence, is here considered. The accurate magnetic field estimation comes from the *IGRF* model [16], while a tilted dipole model (basically stopping the IGRF at the first order coefficient) is also available, to cope with the *IGRF* validity limits (600 km is the maximum altitude considerable).

3.4. Ionospheric Plasma Density

In order to compute the current profile in bare tethers the electron density N_e is required, which is time and space dependent. The following strategy is here applied for the electron density modelling:

- *NeQuick* profiler for the altitude electron density variation;
- data for the profiler acquired off-line in batch mode to build a database exploited in line, during the simulation for the profile generation; data come from the International Reference Ionosphere (*IRI*) model web source at [17].

NeQuick is an analytical profiler, presented in its first version in [18]. The implementation is based on the Epstein layer definition for each ionosphere layer: eq. 2 shows its general formulation, where N is the electron density, h is the altitude, h_m is the altitude of the peak layer, N_m is the peak electron density and b is the layer thickness parameter.

$$N(h; h_m, N_m, b) = \frac{4\,N_m}{\left(1 + e^{\frac{h-h_m}{b}}\right)^2} e^{\frac{h-h_m}{b}} \qquad (2)$$

This model is also part of the *IRI*. The *NeQuick* profiler requires peak frequencies for F_1, F_2 and E layers, and the parameter $M(3000))$ that are time and space dependent. Those inputs, collected off line, are then interpolated to feed *NeQuick* during the simulation runs, whenever needed. Fig. 4 offers an example of the electron density surface wrt height and epoch.

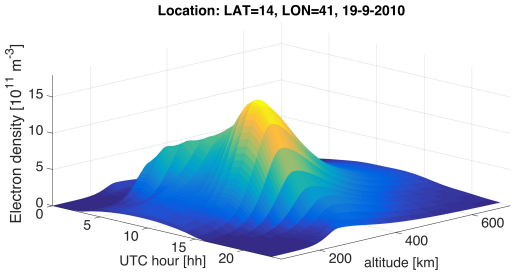

Figure 4. Altitude Profile of N_e, temporal evolution.

4. DESIGN ALTERNATIVES

In order to have a flexible simulator, to explore different design alternatives and options, several degrees of freedom are offered in each involved disciplinary domain, to enlarge the design search domain.
The following configurations and parameters can be set:

- bare versus coated tethers with constant current
- inert tether portions insertion;
- volumetric ratio between conductive and possible reinforcing material in the tether structure;
- tether section shape, round for cables or rectangular for tape tethers;
- deployment direction for bare tethers (for non retrograde orbits the cathode should be closer to the Earth than the anode)
- initial conditions automatically adapted to have equilibrium along the local vertical, or initial amplitude of libration.

5. SIMULATOR VALIDATION

Each implemented model has been validated. The ionosphere complete model is validated against the IRI model: less than 5% error is always present above the maximum density peak; below that value an underestimation usually occurs, leading to an underestimation of the available current; the peak height is however low and usually at such altitudes (between 200-400 km) the current has to be diminished in any case for control reasons.
The overall simulator is validated by comparing the simulation outputs to the available results in literature (e.g. de-orbiting times and rates from [10]) and with analytical checks, whenever available. The former validation showed that general trends always match the results from previous studies. The latter validation is performed by checking, for example, the libration frequency peaks in the in-plane (IP) and out-of-plane (OOP) direction ($\sqrt{3}$ and 2 times the orbital frequency respectively) and the component of the total Lorentz force along the velocity, which must be always negative below geostationary altitude.

6. SYSTEM ARCHITECTURE

An initial simulation campaign is run to identify the most fitting features to design EDT for LEO objects disposal. As confirmed by previous studies (such as [4]), high performance can be achieved by preferring:

- a bare tether, which avoids a massive extra component utilization as for the anodic contactor
- a tape tether, since the large frontal section enhances the electron collection, with respect to a classical round tether
- a small end-mass to exploit for the deployment and possibly containing the cathodic equipment (only downward deployment case)
- as discrete cathodic contactor, if available, either a field emission cathode (FEC) or a hollow cathode (HC), due to the long cathodic segment of tether otherwise required.

Those restrictions are applied to the design for the rest of the discussion.

7. CONTROL

Real satellites, as well as fictitious cases, are considered to verify the suitability of EDT systems and identify their applicability domain; real cases are selected based on their threat as future debris and on the feasibility of EDT systems; the real cases selection is partially based on [19]. The disposal module design is each time tailored for the specific mission, by selecting, for example, tether length and end-mass sizes and masses. For every study case the system proved to be unstable on the long term, therefore an effective control strategy is here proposed, and hereinafter discussed.

7.1. Instability

The instability encountered is a long term phenomenon (few days usually, but always below the total de-orbiting time) for which the complete system libration amplitude becomes very large and leads to tumbling, with a strong loss in the overall dragging efficiency. The system can either remain stuck in an inversed position or start spinning: in any case it experiences large portions of the operational time with cathode and anode reversed with respect to the design condition, not being able to collect current; consequently a strong loss in performance, here quantified in the rate of decay, is experienced. As previously suggested (see [20]) it is found that the instability cause is the continuous positive energy influx in the OOP libration; such energy is then transferred to the IP libration through the non-linear coupling of the dynamics, leading, on the long term, to high libration amplitudes and system tumbling. It is observed, as expected, a faster onset of the instability whenever the longer the tethers, the lower the mass ratio of the end-bodies and the lower the altitudes (i.e. stronger Lorentz forces) are assumed.

7.2. Selected Control

The implemented control is based on the concept introduced in [1] which was never tested on tether representations as accurate as the one developed in the here presented study.
The current control law is settled according to a Lyapunov approach: a non-dimensional stability function V is defined based on estimation of the rotational energy of the system Hamiltonian H, as reported in eq. 3. The quantity H_0 is the rotational energy of the system H at the instantaneous equilibrium, considering only gravitational forces (basically with the tether aligned along the local vertical).

$$V = \frac{H - H_0}{H_0} \tag{3}$$

A threshold V_{TH} is defined a priori for the non-dimensional stability function and the current in the tether is regulated as function of the ratio V/V_{TH}. In this approach the current is left always to flow freely (current equal to the available one) whenever the libration direction and the electrodynamic total torque direction are opposed (Lorentz forces decreasing rotational energy of the system), while it is decreased otherwise depending on V/V_{TH}, as can be seen in fig. 5. The actuation is done either through the variation of the load resistance in the cathode (basically turning Z_l into a varystor), or acting on the voltage difference required by the cathodic emitter (if possible for the selected cathode). The implementation and actuation simplicity

and the low on-board computational cost are the benefits of the proposed control strategy. However, this is a non-optimal but, with a correct threshold selection, it is possible to tend to a minimum de-orbiting time.

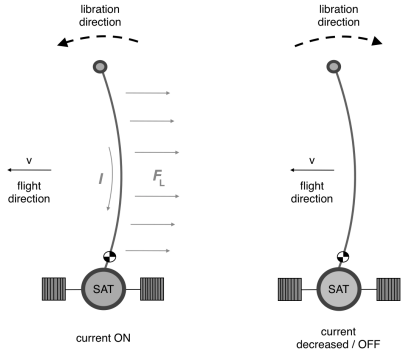

Figure 5. Control scheme activation.

At low altitudes (usually below 600 km) the effects due to gravity gradient and aerodynamic drag, together with the large current variations, impose the use of limitations for the maximum current, together with the control selected. It is found that a value of 1.5 A for the cathodic current threshold is effective for all the study cases, but further analyses should address general rules for the limitation selection.

The control is implemented with several selectable options: the most important concerning the estimation of H (and consequently of V), of the electrodynamic torque and of the libration direction, which can be either computed exactly, taking also into account the tether massive nodes or through an approximation considering only end-masses positions. Lower technology readiness level (TRL) sensors are however required in the former case for a practical application. Whenever the exact description is applied, the considered contributions to H are: kinetic energy, gravitational potential energy, elastic energy (tether elongation) and the term introduced by the non-inertial reference frame. In the case of approximated estimation it is possible to derive analytically H and then V, as done in [2]: the result is reported in eq. 4, where ϕ and θ are the OOP and IP libration angles and ω_0 is the instantaneous orbital angular velocity.

$$V = 4 - 3\cos^2\phi\cos^2\theta\frac{1}{\omega_0^2}\left[\cos^2\phi\left(\dot{\theta}-\omega_0^2\right)+\dot{\phi}^2\right] \qquad (4)$$

Two current regulation algorithms are available: an on-off simple switching and a continuous regulation (see tab.1, where I_{av} is the available current average and I the average current after the control action). In the former case the control strength is tuned by means of α (lower leads to stronger action).

Control method	Condition	Algorithm
on-off	$V/V_{TH} > 1$	$I = 0$
	$V/V_{TH} \leq 1$	$I = I_{av}$
Continuous	$V/V_{TH} > 1$	$I = 0$
	$\alpha < V/V_{TH}$ $V/V_{TH} \leq 1$	$I = I_{av}\cos\left[\frac{\pi}{2}\frac{V-\alpha V_{TH}}{(1-\alpha)V_{TH}}\right]$
	$(V/V_{TH}) \leq \alpha$	$I = I_{av}$

Table 1. Control algorithms

The approximated V is used to define the threshold V_{TH} for all cases, since the analytical expression allows a rough but fast understanding of the libration boundary imposed to the motion, especially for the on-off control method: for example, a value of 0.8 defines a libration contour of 20°/25° for both IP and OOP angles.

7.3. Control Results

The control algorithms implemented have been tested on several real case satellites and their efficiency and effectiveness have been evaluated with respect to the parameters. Two examples are here reported: in the first case a Globalstar-2 satellite is considered, while in the second an EDT system is used to de-orbit a generic Cosmos satellite: tab. 2 reports data for the aforementioned two study cases. The same EDT system is applied to both the cases, data are given in tab. 3, and Z_l and ΔV_{CE} values are used to compute the available current; all perturbations are applied: simple model for atmosphere and dipole model for magnetic field. The starting date for both simulations is 1/1/2013.

Satellite	Unit	Globalstar-2	Cosmos
Mass	[kg]	700	4500
Volume	[m^3]	3.1x2.4x1.5	3x3x7
Semi-major axis	[km]	7778	7378
Eccentricity	[--]	0	0.003
Inclination	[°]	52	64.9

Table 2. Satellite data.

Parameter	Unit	Value/Selection
End-mass	[kg]	15
End-mass volume	[m^3]	0.2x0.1x0.1
Tether length L	[km]	7.5
Tether width w	[cm]	1.2
Tether thickness	[Ω]	0.1
Deployment direction	[--]	downward
Inert fraction	[--]	0
Conductive material	[--]	Al
Reinforcing material	[--]	Dyneema
Conductive/reinforcing material volumetric ratio	[--]	0.5

Cathodic load Z_l	$[\Omega]$	1
Cathodic voltage drop ΔV_{CE}	[V]	50
Tether nodes number	[--]	10

Table 3. EDT system data.

The Globalstar-2 de-orbiting is simulated for 20 days, with no control applied and, then, with the approximated control, with an on-off switching of the current and $V_{TH} = 0.8$ for the stability function. Initial conditions for the tether are assumed at equilibrium, with the EDT aligned to the local vertical. Results are reported in figs. 6-7. As far as no control is applied the semi-major axis variation Δa is $-69.54\ km$, increasing to $-81.25\ km$ if the control is activated. The control is hence efficient in containing the libration and also in increasing the system performance in de-orbiting.

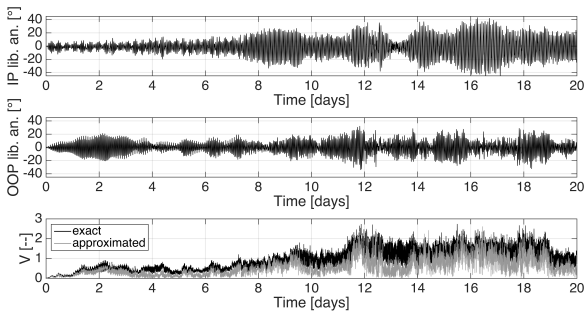

Figure 6. Long term, no control.

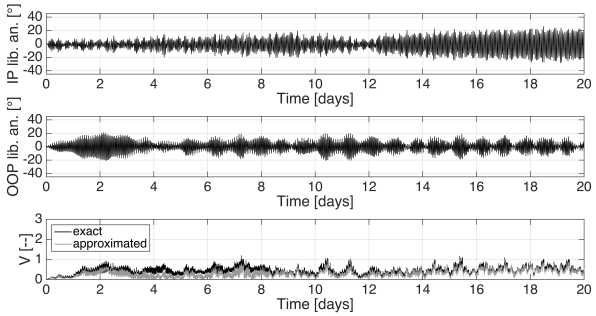

Figure 7. Long term, approximated control.

It can be in fact observed that with no control applied the libration angles are large and the stability function reaches very high values. The motion is instead well bounded within the limits imposed when the system is controlled (see fig. 7).

The de-orbiting of the Cosmos satellite is simulated for 2 days, starting at an altitude of 800 km and with an initial libration of the tether of 25° both IP and OOP. The results with no control are reported in fig. 8, while an exact control with continuous switching, $V_{TH} = 0.8$ and $\alpha = 0.8$, is applied to obtain the results in fig. 9. In this case the control decreases the performance of the system during the 2 days simulation: the de-orbiting rate varies from an average of $-1.75\ km$ per day to $-1.31\ km$. Such result is due to the initial condition far from equilibrium which imposes an initial strong control action. The control is however very effective in reducing the initial motion to a bounded regime.

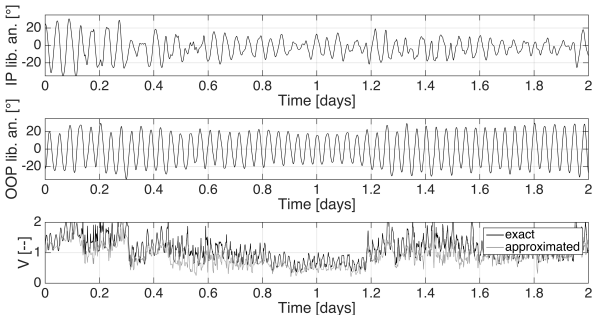

Figure 8. Short term, no control.

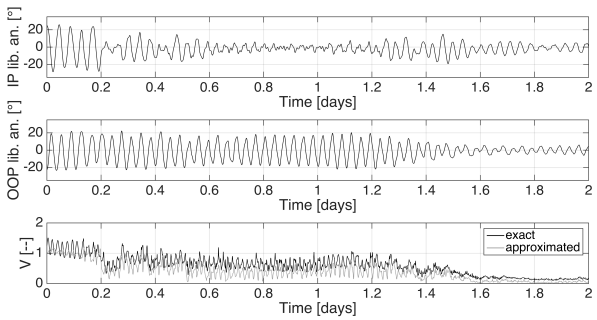

Figure 9. Short term, exact continuous control.

A comparison with other current controls has also been performed: an open-loop control, as proposed in [3], and a control similar to the here developed strategy but with a simpler threshold, as proposed in [5], are compared to an exact on-off control with $V/V_{TH} = 0.8$. The case selected is the de-orbiting of a Globalstar-2 satellite, starting from 800 km altitude to enhance the Lorentz forces; simulation runs for 4 days; tab. 4 offers the control comparison results; *DC* is the duty cycle defined as the percentage of time with average current different from zero. It can be appreciated that the control is needed to avoid the tumbling of the system.

Technique	No control	Exact control	Open -loop	Simple threshold
Tumbling time [days]	3.24	--	--	--
IP/OOP final libration amplitude [°]	--/30	30/7	12/24	50/13
DC [%]	98.8	96	100	43.2
Semi-major axis total variation [km]	-46.4	-60.6	-6.6	-25.9

Table 4. Current control comparison.

The exact control implemented grants a high descent rate and bounded libration. The open-loop control technique is however not efficient and it shows a

continuous libration amplitude growth, probably going to destabilize the system on the long term. The simple threshold control is instead effective in bounding the libration but it is far less efficient with respect to the selected method (see the low duty cycle *DC*).

8. PERFORMANCE DEPENDENCIES

For EDT systems the performance is strongly dependent on the initial orbital conditions. To define an applicability domain and to evaluate initial orbit dependencies, a sensitivity analysis has been performed according to different inclinations and altitudes for a generic 1500 kg satellite. The same EDT system for the Cosmos satellite study case in sec. 7 has been considered, while an exact control with $V_{TH} = 0.8$ coupled with a current limit of 1.5 A is applied. With such a system the stability is granted up to altitudes at which the satellite re-enter is granted in few days, even in case of tether severing. In order to take into account also the tether large cross section, the area-time-product (ATP) of the de-orbiting is considered, as previously done in [10]. Results are compared to those of the same satellite, but decaying due to only atmospheric drag without any tether. The trends obtained are reported in fig. 10.

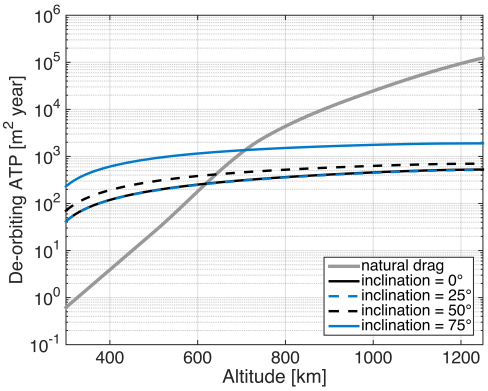

Figure 10. Area-time-product, general case de-orbiting.

The peculiar cosine-like dependence of de-orbiting time on the inclination is observed and similar results are found for inclinations close to the magnetic axis tilt; the latter being 10°, performances of systems in 0° and 25° inclination are similar. The natural drag case delimits the altitude as function of the inclination for which the EDT system starts decreasing the risk of collision during the de-orbiting: the 620 and 700 km interval is identified for the considered system. The system performance strongly depends on the design parameters too, among which the most important are the tether length and width, the deployment direction and the presence of possible inert portions. Two examples are reported to show the influence of the tether length and deployment direction on system stability and performance, always taking into account the control action. The tether length is varied, assuming the disposal scenario of a 1500 kg satellite on a 900 km circular orbit 60° inclined; tab. 3 reports the data for the EDT system adopted, while a continuous approximated control with $\alpha = 0.8$ and $V_{TH} = 0.8$ is applied. Three tether lengths are analyzed: 2.5, 5 and 7.5 km, which lead to a tether mass of 5.5, 11.0 and 16.6 kg respectively; with the 15 kg end-mass, the three EDT systems represent the 1.37%, 1.74% and 2.10% of the total satellite mass. Results in terms of de-orbiting times are reported in fig. 11. The 2.5 km tether is clearly undersized, since a small increase in system mass can lead to a much lower and beneficial de-orbiting duration. Moreover, the analyses lead to state that longer tethers are clearly more unstable, being in any case the control action effective in attaining stability and keeping high de-orbiting rates.

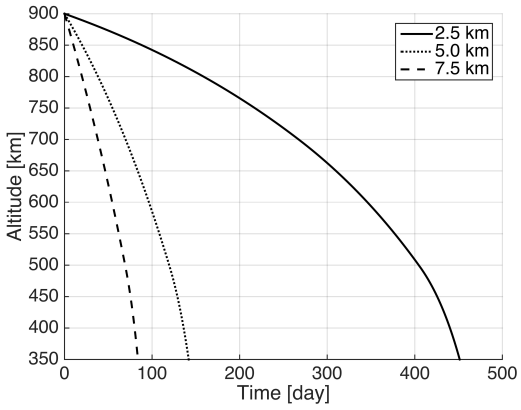

Figure 11. Tether length influence on performance.

The effects of the deployment direction are analyzed on a similar study case as the former: the orbit is slightly varied (800 km circular, 50° inclined), and the exact on-off control with $V_{TH} = 0.8$ is applied. A two days simulation result is reported in fig. 12.

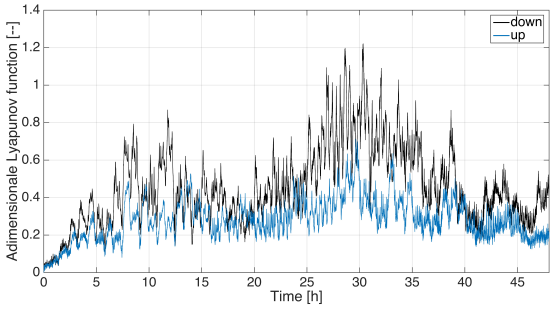

Figure 12. Deployment direction influence on stability.

It can be seen that the upward deployment leads to a more stable system: the control action is not even needed for the first two days, increasing the duty cycle and, slightly, the de-orbiting rate too. The intrinsic higher stability is due to the lower electrodynamic torque (with respect to the system center of mass, higher Lorentz force is closer). The required design for an upward deployment however possibly leads to a higher

total mass, since the end-mass is at the anodic end and it cannot be used to house the cathodic emitter and the other system components (it becomes a dead weight).

9. CONCLUSIONS

A high accuracy versatile simulator for EDT systems performance analysis and design was developed and validated. After a first series of simulations, a most promising configuration was selected to be installed on future satellites for EOL phase control, as a mean of space debris mitigation. The intrinsic instability of the hanging EDT concept was then analyzed and a Lyapunov approach was used to define a current control. More than one possibility was proposed as feasible control law: in particular two main options for the system relevant quantities estimation (e.g. the rotational energy) were addressed. The approximated estimation relies on the observation of only end-bodies position and is usually sufficient to guarantee a stable system, if coupled with the correct control law, threshold selection and current limitation. If the configuration of the tether is also taken into account exact rotational energy estimation is possible: in this case slightly higher effectiveness of the control is possible but, in a practical application, lower TRL sensors are required. The different configuration parameters effect on the system stability was also studied and it was found that longer tether are more effective in disposing satellites, but less stable, and that upward deployment systems should be used if the system mass is acceptable. The selected method for the current profile in non-rectilinear tethers is a critical aspect: an experimental campaign should be done in to validate the implemented model. A future study could also address the current limitation imposed at lower altitudes, in order to find general rules for its selection.

10. Bibliography

[1] N. Takeichi, Practical operation strategy for deorbit of an electrodynamic tethered system, *Journal of Spacecraft and Rockets*, 2006.

[2] J. Corsi and L. Iess, Stability and control of electrodynamic tethers for de orbiting applications, *Acta Astronautica*, 2001.

[3] E. L. M. Lanoix, A. K. Misra, V. J. Modi, and G. Tyc, Effect of Electrodynamic Forces on the Orbital Dynamics of Tethered Satellites, *Journal of Guidance, Control and Dynamics*, 2005.

[4] D. Zanutto, Analysis of propellantless tethered system for the de-orbiting of satellites at end of life, Ph. D. Thesis 2013.

[5] S. Kawamoto, T. Makidab, F. Sasakic, Y. Okawaa, and S. Nishidaa, Precise numerical simulation of electrodynamic tethers for an active debris removal system, *Acta Astronautica*, 2006.

[6] MUST -- Final Report, Department of Aerospace Science and Tecologies, Politecnico di Milano, 2013.

[7] ESA GAST User Manual.

[8] R. Benvenuto, M. Lavagna, A. Cingoli, C. Yabar, and M. Casasco, Must: multi-body dynamics simulation tool to support the GNC design for active debris removal with flexible elements., in *GNC 2014: 9th International ESA Conference on Guidance, Navigation & Control Systems*, Porto, Portugal, 2014.

[9] R. Benvenuto and M. Lavagna, Dynamics Analysis and GNC design support Tool of flexible systems for Space Debris Active Removal, in *2nd IAA Conference on Dynamics and Control of Space Systems (DYCOSS)*, Roma, Italy, 2014.

[10] R. Forward and R. Hoyt, The terminator tether: autonomous de-orbit of leo spacecraft for space debris mitigation, American Institute of Aeronautics and Astronautics, 2001.

[11] J. R. Sanmartin, M. Martinez-Sanchez, and E. Ahedo, Bare wire anodes for electrodynamic tethers, *Journal of Propulsion and Power*, 1993.

[12] C. Bombardelli, J. Peláez, and M. S. Rivo, Asymptotic Solution for the Current Profile of Passive Bare Electrodynamic Tethers, *Journal of Propulsion and Power*, 2010.

[13] R. P. Hoyt, I. M. Barnes, N. R. Voronka, and J. T. Slostad, The Terminator Tape: A Cost-Effective De-Orbit Module for End-of-Life Disposal of LEO Satellites , Tethers Unlimited, Inc., 2009.

[14] J.M. Picone, A.E. Hedin, D.P. Drob, and A. C. Aikin, NRL-MSISE-00 Empirical Model of the Atmosphere: Statistical Comparisons and Scientific Issues, *J. Geophys. Res.*, 2003.

[15] R Panwar, Satellite orbital decay calculations, IPS Radio and Space Services, Australian Government, Bureau of Meteorology, 1999.

[16] C. C. Finlay, S. Maus, C. D. Beggan, T. N. Bondar, and A. Chambodut, International Geomagnetic Reference Field: the eleventh generation, U.S. Department of Commerce,.

[17] [Online]. http://omniweb.gsfc.nasa.gov/vitmo

[18] S. M. Radicella and R. Leitinger, The evolution of the dgr approach to model electron density profiles, *Advances in Space Research*, 2001.

[19] A. Rossi, G. B. Valsecchi, and E. M. Alessi, An evaluation index for the ranking of LEO objects, International Astronautical Congress, 2014.

[20] J. Pelaez, E: C. Lorenzini, O. Lopez-Rebollal, and M. Ruiz, A New Kind of Dynamic Instability in Electrodynamic Tethers , *The Journal of the Astronautical Sciences*, 2000.